ORIGINAL RESEARCH

American Society of Plant Biologists | SEB SOCIETY FOR EXPERIMENTAL BIOLOGY | WILEY

microRNA390 modulates *Nicotiana attenuata*'s tolerance response to *Manduca sexta* herbivory

Maitree Pradhan [ID] | **Catarina Rocha** [ID] | **Rayko Halitschke** [ID] | **Ian T. Baldwin** [ID] | **Shree P. Pandey** [ID]

Department of Molecular Ecology, Max Planck Institute for Chemical Ecology, Jena, Germany

Correspondence
Ian T. Baldwin and Shree P. Pandey, Department of Molecular Ecology, Max Planck Institute for Chemical Ecology, Jena 07745 Germany.
Email: baldwin@ice.mpg.de; shreeppandey@gmail.com

Abstract

miR390 is a highly conserved miRNA in plant lineages known to function in growth and development processes, such as lateral root development, and in responses to salt and metal stress. In the ecological model species, *Nicotiana attenuata*, miR390's biological function remains unknown, which we explore here with a gain-of-function analysis with plants over-expressing (OE-) *N. attenuata* miR390 (Na-miR390) in glasshouse and natural environments. OEmiR390 plants showed normal developmental processes, including lateral root formation or reproductive output, in plants grown under standard conditions in the glasshouse. OEmiR390 plants did not have dramatically altered interactions with arbuscular mycorrhizal fungi (AMF), *Fusarium* pathogens, or herbivores. However, Na-miR390 regulated the plant's tolerance of herbivory. Caterpillar feeding elicits the accumulation of a suite of phytohormones, including auxin and jasmonates, which further regulate host-tolerance. The increase in Na-miR390 abundance reduces the accumulation of auxin but does not influence levels of other phytohormones including jasmonates (JA, JA-Ile), salicylic acid (SA), and abscisic acid (ABA). Na-miR390 overexpression reduces reproductive output, quantified as capsule production, when plants are attacked by herbivores. Exogenous auxin treatments of herbivore-attacked plants restored capsule production to wild-type levels. During herbivory, Na-miR390 transcript abundances are increased; its overexpression reduces the abundances of auxin biosynthesizing *YUCCA* and *ARF* (mainly *ARF4*) transcripts during herbivory. Furthermore, the accumulation of auxin-regulated phenolamide secondary metabolites (caffeoylputrescine, dicaffeoylspermidine) is also reduced. In *N. attenuata*, miR390 functions in modulating tolerance responses of herbivore-attacked plants.

KEYWORDS
ARF4, auxin, herbivore resistance, *Manduca sexta*, miR390, *Nicotiana attenuata*, tolerance, YUCCA

1 | INTRODUCTION

microRNAs (miRNAs) form an essential layer of regulators of gene expression in nearly all eukaryotes. They are noncoding RNA molecules, produced from the stem regions of hairpin precursor molecules. miRNAs are produced from "miRNA genes" in an RNA-polymerase II dependent manner (Song et al., 2019). Most miRNA genes are found in intergenic regions and are transcribed as independent units. Several miRNAs are also intronic and cotranscribed with their host protein coding regions (Song et al., 2019). The size of mature miRNAs ranges from 18–25 nucleotides (nt), with 21–22 nt long miRNAs being the most abundant in plants. miRNAs recognize their targets through sequence complementarity, where they facilitate mRNA cleavage, translational repression, and DNA methylation (Pandey et al., 2019; Song et al., 2019). miRNAs are thought to play indispensable roles in a plant's phenotypic plasticity, being involved in the regulation of differentiation, development and reproduction, and mediating responses to environmental fluctuations (Brant & Budak, 2018; Li et al., 2017; Song et al., 2019). In studies that have manipulated the expression of different components of the small-RNA (smRNA) pathways, evidence for roles in the diverse plastic responses that allow plants to adapt to environmental challenges in natural habitats has been reported (Pandey et al., 2008; Pandey & Baldwin, 2007; Pradhan et al., 2017, 2020).

The effectors of miRNA action, the Argonaute (AGO) proteins, are conserved across all lineages of photosynthetic organisms (Pradhan et al., 2020), indicating that miRNA-driven regulation of gene expression could be ancient. However, individual miRNAs/miRNA-families appear to evolve rapidly, as suggested by their frequent birth and loss in lineage- and species-specific manners (Cuperus et al., 2011; Nozawa et al., 2012). Most miRNA genes appear to be relatively young (Cuperus et al., 2011), and only a few miRNA families are conserved across plant lineages (Cuperus et al., 2011; Nozawa et al., 2012). miRNA390 (miR390) is one of these, being highly conserved across lineages of vascular and nonvascular plants (Morozov et al., 2018; Xia et al., 2017). Studies focusing on evolution of miR390 have highlighted significant variations in its regulatory circuit (Xia et al., 2017). Yet, the exploraiton of diversification of miR390 biological functions has remained limited.

At a molecular level of analysis, miR390 acts as an activator of the trans-acting small interfering RNA (tasiRNA) pathway, with two known target sites in the transcript of the tasiRNA precursor gene, TAS3 (Axtell et al., 2006). Following miR390-directed cleavage, tasiRNAs are produced from TAS3 transcripts, which regulate auxin response factors (ARFs). ARFs are a class of transcription factors that modulate (repressing or activating) the expression of genes regulated by the plant hormone, auxin. In this way, miR390 functions as a central component of the highly conserved "miR390-TAS3-ARF regulatory pathway" (Xia et al., 2017), which is expected to modulate auxin signaling. In turn, in Arabidopsis, miR390 expression itself is regulated by auxin levels (Yoon et al., 2010).

miR390 has been regarded as a key regulator of developmental events in several plant species. miR390 has been described to mediate lateral root growth, developmental timings, and patterning in Arabidopsis and *Physcomitrella patens* (Cho et al., 2012; Marin et al., 2010). During potato development, miR390 regulates a calcium-dependent protein kinase (CDPK) that phosphorylates auxin efflux carriers (Santin et al., 2017). Interestingly, miR390 has also been implicated in abiotic stress responses, in particular, salt and metal stress, by regulating lateral root growth (Ding et al., 2016; Dmitriev et al., 2017; He et al., 2014, 2018; Lu et al., 2018). The miR390/TAS3 regulatory module also plays an important role in gall formation when Arabidopsis roots are attacked by the nematode *Meloidogyne javanica* (Cabrera et al., 2016). Infection by root-knot nematodes induces the expression of miR390/TAS3 smRNA, which is necessary for gall formation, possibly through ARFs (Cabrera et al., 2016). Legume root colonization by symbiotic rhizobia also requires the regulatory miR390/TAS3 module to control rhizobial root colonization and nodule formation. Overexpression of miR390 promotes lateral root growth while negatively regulating nodule organogenesis, rhizobial infection, and induction of nodulation signaling pathway (NSP) 1 and 2 genes (Hobecker et al., 2017). These studies indicate a role of miR390 not only in developmental processes but also during different stress responses and symbiotic interactions. However, the role of miR390 in modulating host responses to other stress factors, such as pathogen and herbivore attack, as well as interactions with arbuscular mycorrhizal fungi (AMF) have not been thoroughly studied. Moreover, the functional role of miR390 has not been examined in plants growing in their natural habitats.

Nicotiana attenuata is an annual plant native to the southwestern United States and is an ecological model as its natural history and its interactions with herbivores, pollinators, and microbes have been extensively studied not only under glasshouse conditions but also in its natural habitats (Baldwin, 2001; Navarro-Quezada et al., 2020). This wild tobacco species grows in the agricultural primordial niche: the post-fire habitat. After wild fires, *N. attenuata* germinates from long-lived seed banks and establishes mono-culture populations, while encountering several ecological challenges. The plant is colonized by AMF (Pandey et al., 2018) and is also attacked by pathogens such as *Fusarium* and *Alternaria* species (Schuck et al., 2014). Furthermore, *N. attenuata* faces an unpredictable attack by a diverse suite of herbivore species, which is thought to represent an important ecological challenge for this species; consequently, *N. attenuata* recruits several direct and indirect defenses (Baldwin, 2001; Navarro-Quezada et al., 2020). Additionally, *N. attenuata* has a remarkable capacity to tolerate herbivore attack to minimize fitness losses (Schwachtje et al., 2006). *N. attenuata*'s resistance and tolerance strategies, the signaling cascades, and defense-related secondary metabolites have been well studied. Moreover, the composition and role of the RNA-directed RNA polymerase (RdR), DCL, and AGO components of the smRNA machinery during adaptation to these natural challenges have also been studied (Navarro-Quezada et al., 2020). The composition of miRNAs in *N. attenuata's* genome (Xu et al., 2017) and its reprograming during herbivore attack, pathogen infection, and AMF colonization are also known (Pandey et al., 2018; Pradhan et al., 2017, 2020).

miR390 has been identified in *N. attenuata*; its expression is up-regulated during simulated herbivory (Bozorov et al., 2012), whereas it is down-regulated during interactions with AMF (Pandey et al., 2018). Yet, the biological function of this highly conserved miRNA remains poorly studied in *N. attenuata* and is the subject of this investigation. We performed gain-of-function studies by stable over-expression (OE-) of *N. attenuata* miR390 (Na-miR390) to evaluate changes in performance when plants engage with other organisms, specifically, with AMF, a native pathogen (*Fusarium brachygibbosum*) and a native herbivore (*Manduca sexta*).

2 | RESULTS

2.1 | miR390 does not regulate development events in *N. attenuata*

In *N. attenuata*, miR390 sequences have been reported in two previous independent investigations (Bozorov et al., 2012; Pandey et al., 2018). Na-miR390a-i (Bozorov et al., 2012) and Na-miR390-5p-ii (Pandey et al., 2018) are nearly identical as they vary in only a single nucleotide (A/G) at the 19th position of the mature sequence (Figure S1). We compared the *N. attenuata* miR390 sequences to those of other species (Figure S1). Both sequence variants have been reported in other plant species: For instance, Gm-miR390 contains an "A" at 19th position, whereas Mt- and At-miR390s contain the "G" (Figure S1). As there are no variations in 20 of 21 nucleotides, including the important residues of target recognition and cleavage site within the first 12 nucleotides, we do not expect significant effects of this single nucleotide variation in the regulation of targets of this miRNA.

To evaluate the biological function of this miRNA, we over-expressed the originally identified Na-miR390a-i in transgenic lines (OEmiR390) with the transformation vector shown in Figure S1 that carries the miRNA sequence as well as backbone sequence. After transformation, we obtained 20 independently transformed lines and screened them for homozygosity, occurrence of single insertions, completeness of the insertions (no truncations or border over-reads), and successful overexpression. For further experiments, we selected two homozygous lines, A-12-392-63-71 and A-12-385-42-51, which showed strong overexpression and harbored a single complete insertion (Figures 1a and S1).

Based on previous results for lines altered in miR390 expression (Marin et al., 2010), we measured seedling root lengths and the number of lateral roots (Figure 1b). No significant reductions in root length (one-way ANOVA, $F = .621$, $P > .05$) were observed for the two *N. attenuata* lines overexpressing miR390. Furthermore, in contrast to the results of studies with other plant species (e.g., rice (Lu et al., 2018) and Arabidopsis (Marin et al., 2010)), the number of lateral roots in OEmiR390 *N. attenuata* plants was also not significantly altered (one-way ANOVA, $F = .65$, $P > .05$) as compared to those of WT seedlings (Figure 1b).

As miR390 is thought to play a key role in the juvenile-to-adult phase transition of many species, we grew the two

miR390-overexpressing lines in individual pots with full nutrient supply and documented growth parameters indicative of changes in phase transitions. The two OEmiR390 lines did not show any significant differences in rosette size (one-way ANOVA, $F = 1.17$, $P > .05$), stalk length (one-way ANOVA, $F = 2.91$, $P = .183$), flower (one-way ANOVA, $F = 1.228$, $P > .05$) and capsule numbers (two-way repeated measures ANOVA with Bonferroni correction, $F = 1.87$, $P > .05$ and Kruskal–Wallis test) when compared with WT plants (Figure 1c,d). These results indicated that overexpression of miR390 does not dramatically change plant development or fitness in *N. attenuata* under standard, unstressed growth conditions of the glasshouse.

2.2 | Na-miR390 does not affect resistance, colonization, or reproductive output during plant-pathogen and plant-AMF interactions in *N. attenuata*

Previous studies have reported that the expression of miR390 is altered during a plant's interaction with microbes (Hobecker et al., 2017; Pandey et al., 2018), and this motivated our search for its roles in plant-AMF and plant-pathogen interactions. To examine if miR390 is a crucial factor for AMF root colonization, similar to its role in symbiotic nodulation in legumes (Hobecker et al., 2017), we inoculated plants grown under reduced inorganic phosphate (Pi) fertilization regimes with AMF, observed growth and development, and determined root AMF colonization by measuring the levels of 11-carboxyblumenol–C glucoside in leaves as a proxy for AMF colonization (Wang et al., 2018). Blumenol levels were not significantly different among the WT and miR390-overexpressing lines (Figure 2a). Furthermore, rosette diameters, flower and capsule numbers were not different between WT and OEmiR390 plants (Figure S2). Only stalk lengths were marginally higher for one of the two lines (Figure S2). Similar results were obtained for plants grown individually in 1 L pots as well as for OEmiR390 plants competing with an initially size-matched WT neighbor (Figure S2). The marginal increase in stalk length had no fitness consequences as seed capsule production did not differ between the WT and the miR390 overexpressing plants.

To evaluate if Na-miR390 is involved in the resistance response to a natural fungal pathogen, single leaf inoculations with *Fusarium brachygibbosum* Utah 4 isolates were performed (Pradhan et al., 2020), and the development of visible disease symptoms was recorded. No significant differences in the diameter of chlorotic/necrotic lesions of WT and miR390-overexpressing plants were observed during infection with the *Fusarium* pathogen (Figures 2b and S3).

These results suggest that Na-miR390 does not play a significant role in these plant-fungal (pathogen and AMF) interactions.

2.3 | Na-miR390 has a role in host tolerance response during herbivory

miR390 transcripts accumulate 1 h after simulated herbivory in *N. attenuata* (Bozorov et al., 2012). We confirmed this upregulation of
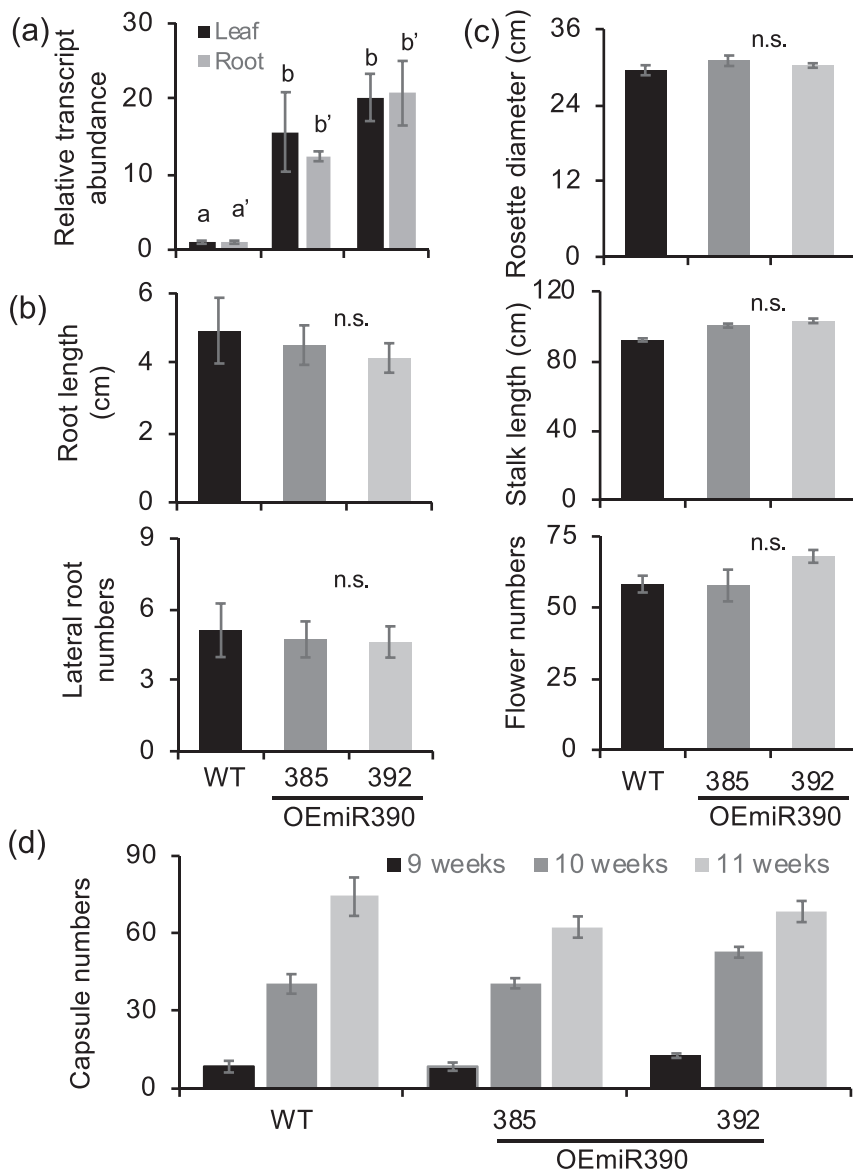
FIGURE 1 Phenotypic characterization of two independent, homozygous OEmiR390 lines (392, 385). (a) miR390 was overexpressed in *N. attenuata* (OEmiR390 plants) in two independent lines. Wild type seeds and seeds of the two OEmiR390 lines (392, 385) were germinated on GB5 medium. Transcript accumulation of miR390 was analyzed in 10 day-old seedlings by qPCR with miR390 specific primers ($N = 3$, mean $\pm$ SE). Different letters indicate significant differences based on one-way ANOVA with Tukey's HSD. (b) The two lines do not differ in root length and the number of lateral roots 10 days after germination ($N = 5$–6, mean $\pm$ SE). Each replicate represents 5 pooled seedlings from an independent GB5 germination Petri dish. n.s., no significant difference among the lines based on ANOVA analyses, $p > .05$. (c) Growth and (d) fitness data were recorded of non-treated OEmiR390 and WT plants grown under glasshouse conditions in potting soil. Stalk lengths, rosette diameters and flower numbers were taken after 9 weeks, and capsule numbers after 11 weeks ($N = 4$, mean $\pm$ SE). n.s., no significant difference based on ANOVA and Kruskal–Wallis test
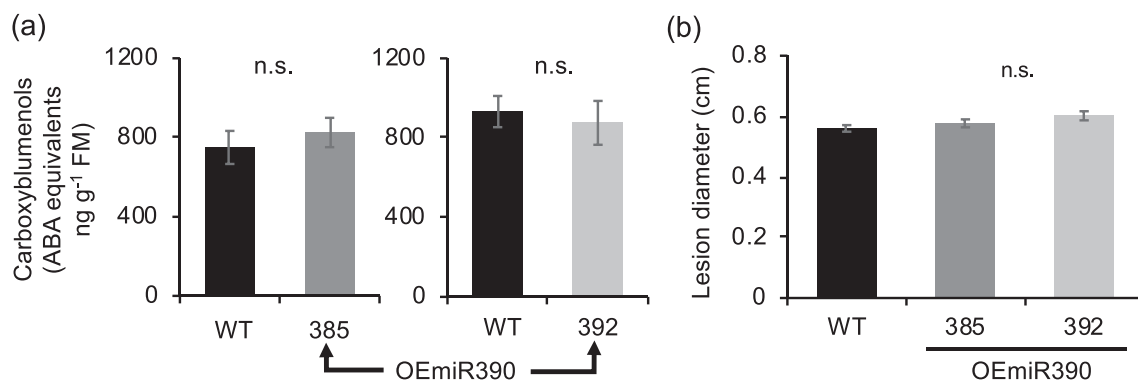

FIGURE 2 miR390 does not play a role in arbuscular mycorrhizal root colonization, or in pathogen defense in *N. attenuata*. (a) The two lines overexpressing miR390 (392, 385) were grown in 2 L pots in competition with wild type (WT) plants with AMF inoculum and the levels of leaf 11-carboxyblumenol-C glucoside as marker of arbuscule colonization were measured 6 weeks after inoculation ($N = 8$–9, mean $\pm$ SE). (b) In rosette-stage plants grown individually in 1-L pots, leaves were infiltrated with a spore suspension of *F. brachygibbosum*. Lesion diameters were measured and photographed 7 days after infection ($N = 10$, mean $\pm$ SE); n.s., no significant difference based on ANOVA analyses

Na-miR390 in leaf samples harvested 1 h after wounding and application of *M. sexta* oral secretion (simulated herbivory) in WT plants, while the expression was not further enhanced in the overexpressing lines (Figure 3a). To examine Na-miR390's functional role in plant–herbivore interactions, we used two established approaches to evaluate both- the herbivore and plant sides of the interaction: (i) We measured the growth of *M. sexta* larvae feeding on WT and the two lines overexpressing Na-miR390. This "caterpillar performance bioassay" evaluates if the defenses and/or nutritional capacity of host plants is altered (Pandey & Baldwin, 2007; Pradhan et al., 2017). (ii) We recorded plant growth and reproductive output/plant fitness in WT and OEmiR390 plants during herbivory. The maintenance of reproductive output in herbivore-attacked plants reflects a plant's tolerance of herbivore attack (Schwachtje et al., 2006).

(i) Caterpillar growth was not affected when consuming Na-miR390 overexpressing plants. Independent of plant genotype, *M. sexta* 1st to 4th instar caterpillars gained equivalent amounts of mass (two-way repeated measures ANOVA, $F = .224$, $P = .78$) when feeding on WT and OEmiR390 plants (Figures 3b and S4). They also

appeared to consume similar amounts of plant material from both the genotypes (Figure S4).

(ii) *M. sexta*-damaged OEmiR390 plants had taller stems than similarly damaged WT plants (one-way ANOVA with Bonferroni correction, $F = 15.60$, $P = .00008$; Figure 3c). However, herbivore-damaged OEmiR390 plants produced significantly fewer seed capsules (one-way ANOVA, $F = 5.68$, $P < .01$ and Kruskal-Wallis test followed by Dunn's test) than did WT plants (Figure 3d), a decline seen in both the number of open and closed capsules (Figure S4). Independent feeding experiments confirmed these results (Figure S4). The significant reductions in capsule production of attacked plants suggested that miR390 expression influences *N. attenuata*'s tolerance of herbivory.

2.4 | Overexpression of miR390 reduces the accumulation of auxin and auxin-regulated phenolamides during herbivory

To further understand the physiological basis of reduced herbivore tolerance of OEmiR390 plants, we quantified phytohormone levels in
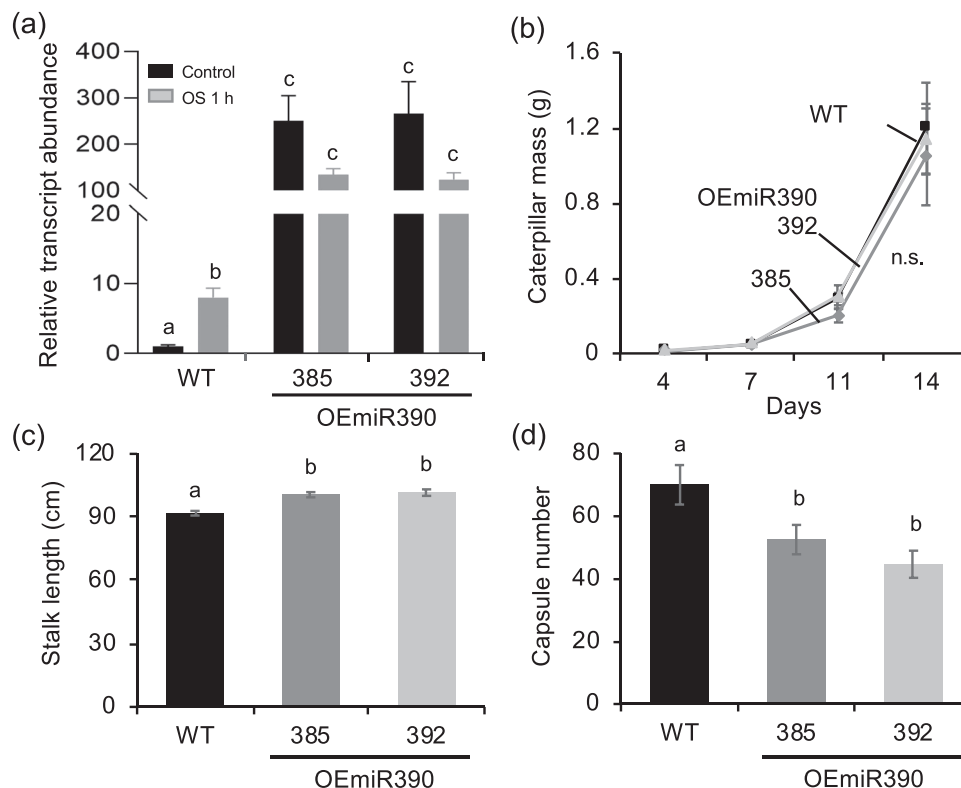

FIGURE 3 Caterpillar growth is not affected by miR390 overexpression, but seed capsule production is impaired in OEmiR390 plants after herbivory. (a) Expression of miR390 in WT and two lines overexpressing miR390 after simulated herbivory (OS: oral secretions of *Manduca sexta* larvae added to puncture wounds) was analyzed by qPCR of leaves 1 h after treatment with OS and untreated control leaves ($N = 3$–4, mean ± SE). Different letters indicate significant differences based on ANOVA with Tukey's HSD. (b) 1st instar larvae were placed on rosette stage plants and caterpillar growth was quantified for 14 days ($N = 8$–22, mean ± SE); n.s., no significant difference based on ANOVA analyses. (c) Stalk lengths and (d) the number of capsules was determined 11 weeks after potting ($N = 7$–8, mean ± SE). Different letters indicate significant differences based on ANOVA with Bonferroni correction for stalk length and Kruskal–Wallis test with Benjamin–Hochberg followed by Dunn's test for capsule numbers

response to caterpillar feeding. Insect attack changes the accumulation of a suite of phytohormones that includes jasmonates, salicylic acid (SA), abscisic acid (ABA), and auxin. Auxin modulates herbivore-induced tolerance-defense trade-offs (Machado et al., 2013; Machado et al., 2016) along with jasmonates that also regulate induced plant defenses during herbivory (Howe & Jander, 2008). Auxin levels were significantly reduced (by up to nine-fold: to 10.6% and 28.8% of WT levels for lines 385 and 392, respectively) in herbivore attacked OEmiR390 plants as compared to WT plants (Figure 4a). In contrast, levels of jasmonic acid (JA) and its active conjugate, jasmonoyl-isoleucine (JA-Ile), did not significantly differ between the two OEmiR390 lines and the WT during herbivory (Figure 4a). Furthermore, SA and ABA levels were also not significantly different between the OEmiR390 and the WT plants (Figure S5).

Auxin regulates the accumulation of phenolamides, such as caffeoylputrescine and dicaffeoylspermidine, during herbivory (Machado et al., 2016). The reduced auxin accumulations in OEmiR390 plants during herbivory motivated us to investigate whether these metabolites were also affected. Indeed, both metabolites were significantly reduced in herbivore-damaged OEmiR390 plants as compared to the WT (Figure 4b). From these results, we infer that overexpression of miR390 specifically inhibits the accumulation of auxin and auxin-regulated metabolites during herbivore attack.

Additionally, we determined how the expression of *GAL83* was affected by miR390. GAL83 is a regulatory subunit of an SnRK1-related kinase that is involved in plant tolerance to herbivory by regulating source-sink relationship of carbon assimilates (Schwachtje et al., 2006). No differences were observed in *GAL83* levels in WT and OEmiR390 plants during herbivory (Figure 4c), or during constitutive conditions (no-herbivory controls; Figure S6).

2.5 | Exogenous application of IAA restores tolerance to herbivory

The reduced accumulations of auxin as well as auxin-regulated phenolamides suggested that auxin was the critical factor in the reduced tolerance of OEmiR390 to herbivory. To test this hypothesis, we determined how the complementation of herbivore-attacked plants with exogenously supplied auxin (indole acetic acid [IAA], 1 mM as a lanolin paste to petioles) effects the plant's reproductive performance. Indeed, when treated with exogenous IAA, herbivore-attacked OEmiR390 plants were able to restore their capsule production to the WT levels (Figure 5). The OEmiR390 plants that were fed by only *M. sexta* for 9 continuous days (no IAA complementation; feeding controls) had reduced capsules as compared to similarly attacked WT plants (Figure 5), whereas no differences in capsule productions were seen among the three lines when no herbivore stress (no-herbivory treatment controls) was applied (Figure 5). Both of these control datasets are consistent with the observations described above.

2.6 | Overexpression of miR390 down-regulates expression of auxin biosynthesis (*YUCCA*) and auxin response factor (*ARF*) genes during herbivory

The rate-limiting step in auxin biosynthesis involves oxidative decarboxylation of indole-3-pyruvic acid (Figure 6). This reaction is catalyzed by the flavin monooxygenase-like proteins encoded by *YUCCA* genes (Machado et al., 2016). Expression of *YUCCA* genes, like *YUCCA1* and *YUCCA3*, is elicited quickly within 60 min of simulated *M. sexta* attack in *N. attenuata* (Machado et al., 2016). We evaluated how the expression of these *YUCCA* genes were altered after overexpression of Na-miR390. OEmiR390 plants accumulated significantly fewer transcripts of *YUCCA1* (reductions by 50% of WT levels) and *YUCCA3* (reductions by 52%) during herbivory (Figure 6). No differences in constitutive levels (in no-herbivory controls) were observed between the WT and OEmiR390 plants (Figure S6).

ARFs are a demonstrated target of the miR390/TAS3 pathway, which modulate auxin signaling. Furthermore, ARFs, specifically ARF4 (Marin et al., 2010; Yoon et al., 2010), also often have feedback/homeostatic roles for miR390 expression during auxin signaling. Therefore, we analyzed the accumulation of *ARFs* in the Na-miR390 overexpression lines, 9 days after continuous herbivore feeding. The up-regulation of miR390 correlated with a down-regulation of *ARFs*, in particular of *ARF4* (Figure 7): the levels of *ARF4* mRNA were significantly down-regulated (by up to 3-fold reductions in comparison to the levels of WT plants) in herbivore-damaged OEmiR390 plants, whereas reductions in *ARF2* were more modest and those of *ARF3* were only marginally lower (Figure 7). The constitutive transcript levels of *ARFs* in the uninduced WT and the OEmiR390 plants were similar (Figure S6). These results were consistent with the inference that overexpression of miR390 had down-regulated ARF expression and auxin signaling during herbivory.

Overall, we infer that miR390 in *N. attenuata* plays a central role in optimizing plant fitness/tolerance responses during *M. sexta* herbivore attack by modulating auxin signaling (Figure 8).

2.7 | Performance of OEmiR390 plants under natural conditions

The biological function of any miRNA has yet to been examined under field conditions. Our two decade long experience of planting transgenic plants into natural habitats has revealed that some phenotypes only become apparent when plants are grown under field conditions (Kessler et al., 2004), while other phenotypes, clearly seen in the glasshouse, are lost in the field, due to the multiplicity of environmental signals that plants are exposed to under natural conditions (Kaur et al., 2012). We therefore planted one of the miR390 overexpressing lines in the plant's native habitat (in the Great Basin Desert of Utah, USA) in the 2019 field season, in size-matched pairs with WT plants and observed herbivore damage as well as growth and fitness parameters for 8 weeks of growth in the field. Rosette diameters were similar between the WT and the OEmiR390 plants (repeated measures
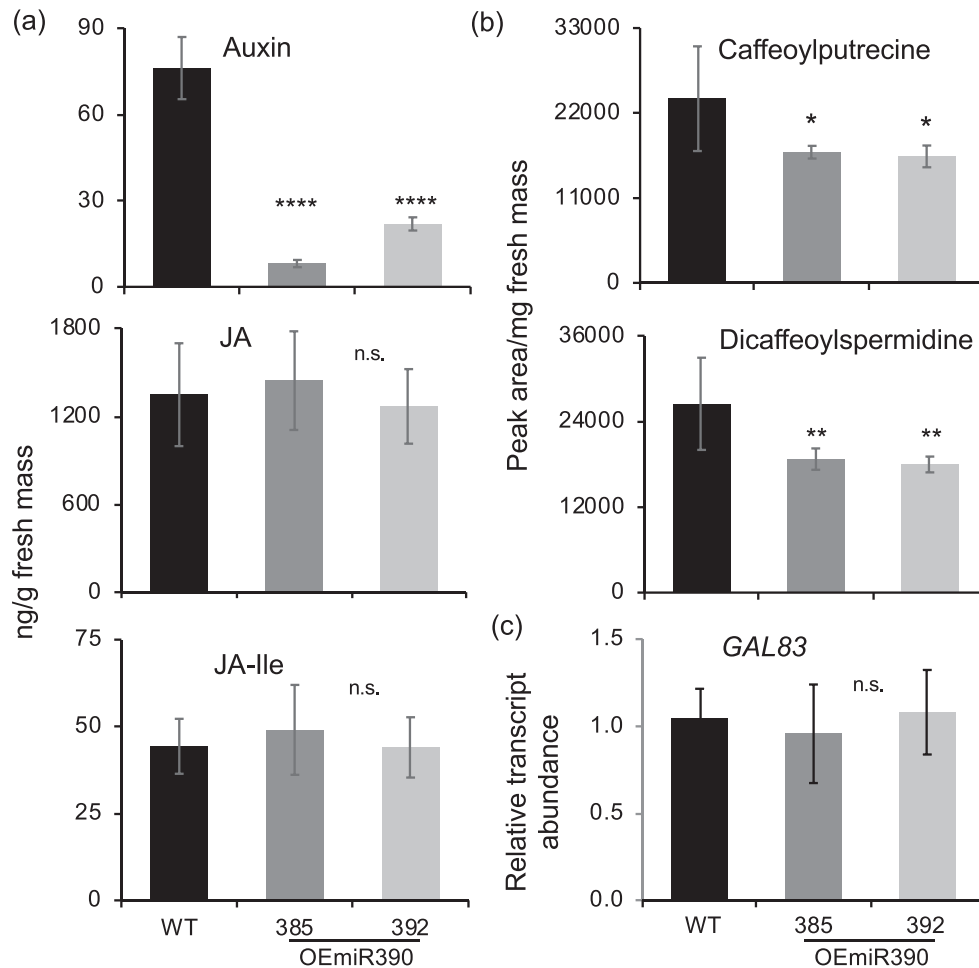
PRADHAN ET AL.

American Society
of Plant Biologists

S-E-B
SOCIETY FOR EXPERIMENTAL BIOLOGY

WILEY | 7 of 14

FIGURE 4 Overexpression of miR390 reduces the production of auxin and auxin-dependent tolerance responses but not jasmonates during herbivory. (a) Levels of auxin, jasmonic acid (JA) and JA-isoleucine (JA-Ile) hormones were quantified in plants continuously fed on by *M. sexta* for 9 days. Auxin levels were strongly attenuated in miR390-overexpressing plants; one-way ANOVA, $F = 43.17$, $n = 10$–15, **** significantly different at $P < .001$. n.s., no significant differences in JA or JA-Ile amounts were observed between WT and OEmiR390 plants. (b) Evaluation of factors related to tolerance response of *N. attenuata* during herbivory. Peak areas of caffeoylputrescine (upper panel) and dicaffeoylspermidine (middle panel). Levels were measured in the leaves after 9 d of *M. sexta* feeding. One-way ANOVA, $F = 1.8$ for caffeoylputrescine and $F = 4.54$ for dicaffeoylspermidine. $n = 10$–15, * and ** represent significant differences from WT at $P \leq .05$ and $P \leq .01$. (c) Lower panel shows transcript abundance of GAL83 after 9 days of *M. sexta* feeding on WT and two miR390 overexpressing plants. No significant differences among genotypes were observed

ANOVA, $n = 17$, $F = 2.36$, $P = .115$), while stalk lengths of OEmiR390 plants were marginally taller than WT plants (repeated measures ANOVA, $n = 17$, $F = 10.702$, $P = .0395$) at the end of the field season (Figure S7). Overall, the WT and the OEmiR390 plants encountered mild attack rates from the natural herbivore community, resulting in only 10%–12% losses of rosette area after 3 and 4 weeks, which decreased to nearly 7% for the rest of the season. When herbivore damage (at 4 weeks after planting) was correlated with the number of capsules, OEmiR390 plants exhibited a steeper decline in capsule numbers at the higher early herbivore damage rates (Figure S7). It should be noted that for the 2019 field season, *Manduca* species did not arrive while the OEmiR390-WT plant pairs were in the field.

3 | DISCUSSION

Here, we examined the biological function of miR390 in the ecological model plant species, *N. attenuata*. We show that Na-miR390 plays a role in modulating tolerance responses during *M. sexta* attack, likely by regulating auxin signaling, but does not play a major role when plants are colonized by beneficial or pathogenic fungi. Overexpression of Na-miR390, one of the highly conserved plant miRNAs, resulted in reduced plant reproductive output only when plants were attacked by *M. sexta* caterpillars. The overexpression of miR390 did not significantly influence caterpillar performance (caterpillar mass), and also did not significantly influence plant development or its reproductive output when grown under unstressed glasshouse conditions.
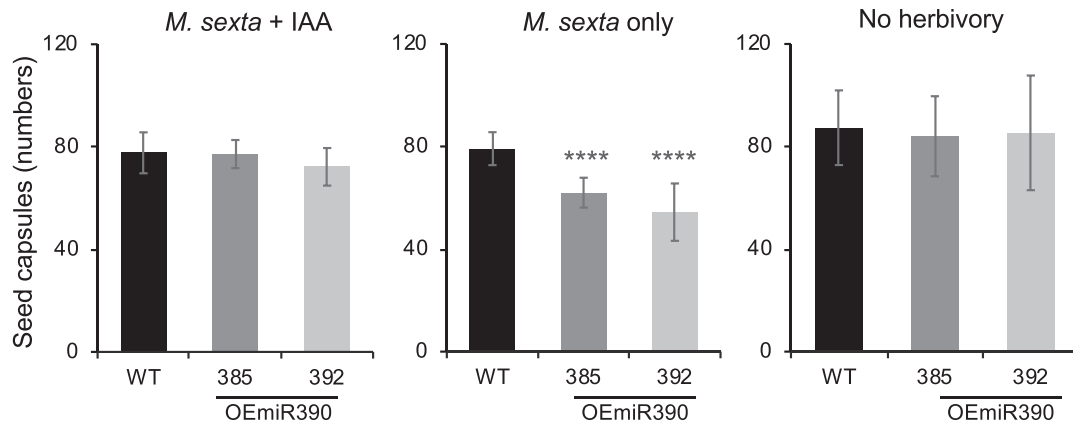
FIGURE 5 Exogenous application of IAA restores plant fitness during herbivore attack. No significant difference in capsule production between the WT and the two lines of OEmiR390 was observed when plants attacked by *M. sexta* larvae were exogenously supplied with 1 mM IAA in lanolin paste (left panel). Whereas the middle and the right panels represent the feeding and no-feeding controls: highly significant reductions in plant fitness (middle panel; one-way ANOVA, $F_{2,14} = 14.42$, $P < .0005$, indicated by ****), measured as seed capsule production, was observed in miR390-overexpressing plants (OEmiR390) compared to WT when continuously attacked by *M. sexta* caterpillars (1 per plant) for 9 days. No difference in capsule production was observed between transgenic and WT genotypes when plants were not attacked by herbivores
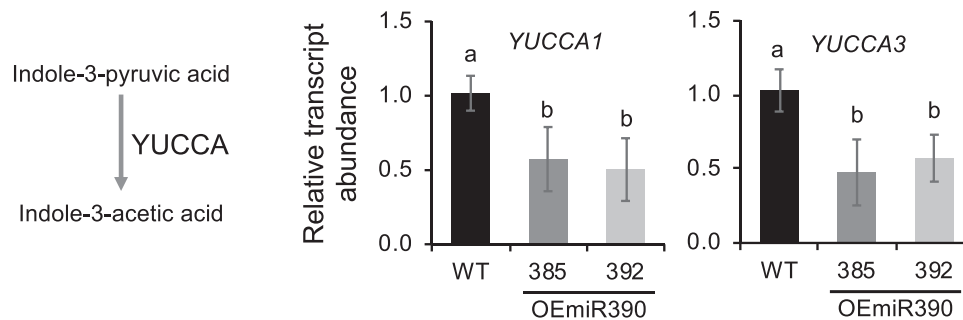

FIGURE 6 miR390-overexpression reduces transcript accumulation of auxin biosynthesizing *YUCCA* genes during simulated herbivory. Conversion of indole-3-pyruvic acid to indole-3-acetic acid marks the rate-limiting step in auxin biosynthesis and is catalyzed by YUCCAs (left panel). Single leaves (+2 position) of wild type (WT) and miR390-overexpressing plants (OEmiR390; lines 385 and 392) were subjected to simulated herbivory (puncture wounding and application of *M. sexta* oral secretions), and after 60 min, leaves were harvested for evaluating transcript abundances of *YUCCA1* and *YUCCA3* genes with quantitative real-time PCR assays. Transcript levels in WT were set to 1 and relative abundances in the two OEmiR390 lines were determined. *ECI* was used as internal reference; 4 biological replicates were used. Error bars represent mean ± SDs. Significant reductions in *YUCCA1* (one-way ANOVA, $F = 3.84$, $P < .05$) and *YUCCA3* (one-way ANOVA, $F = 2.12$, $P < .05$) in both the OEmiR390 lines were recorded. (a) and (b) indicate statistically significant differences between the genotypes

We propose the following model for the ecological role of miR390 in modulating host tolerance responses to herbivory (Figure 8): attack of *M. sexta* larvae elicits an auxin burst (Machado et al., 2013, 2016) parallel to the elicitation of jasmonates. The attack also elicits miR390 expression, which regulates auxin biosynthesis (such as YUCCA gene expressions), its levels and the expression of ARFs (e.g., *ARF4*), which, in turn, modulates auxin-responsive changes in secondary metabolism and tolerance responses (Figure 8). This miR390-auxin regulated tolerance response is independent of (and plausibly synergistic to) JA and GAL83 (Schwachtje et al., 2006) regulations (Figure 8). Whether the miR390-ARF4-auxin module mediates the oft-discussed tolerance-defense tradeoffs during herbivory in *N. attenuata* requires additional research.

Tolerance of plants to insect attack is a distinct type of response to herbivory, yet little is known about its mechanistic basis (Koch et al., 2016). Tolerance is characterized as a host plant's ability to recover from injuries of herbivore attack through compensatory physiological processes (Koch et al., 2016). Resistance to insect attack is often categorized into antibiosis (traits that impact pest biology), antixenosis (non-preference traits impacting pest behavior), and tolerance. Tolerance is distinctive from the other two types of resistance as these traits do not necessarily interfere with the performance (growth, physiology, behavior, or population) of the attacking insects but only reduce the fitness impact of herbivory on the host after it has occurred (Koch et al., 2016). In agro-ecological terms, tolerant plants are able to maintain their fitness to a greater degree when
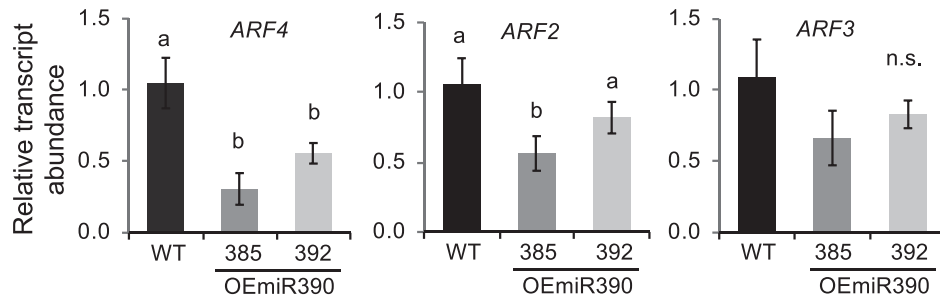
FIGURE 7 Overexpression of miR390 down-regulates accumulation of transcripts of auxin response factors (*ARFs*) during herbivory. After 9 days of caterpillar feeding, transcript abundances in WT and the two miR390 overexpressing lines (OEmiR390) were evaluated with quantitative real-time PCR assays. *ECI* was used as internal reference. Transcript levels in WT were set to 1 and relative abundances in the two transgenic lines were determined. Four biological replicates were randomly chosen; values represent mean $\pm$ SDs. Transcripts of *ARF4* were significantly down-regulated in both the miR390-overexpressing lines (one-way ANOVA, $F = 7.032$, $P < .01$). Down regulation of *ARF2* was significant in one of the OEmiR390 lines (one-way ANOVA, $F = 3.296$, $P_{WT,392} < .05$), whereas there were no significant differences (n.s.) in *ARF3* levels among the three genotypes. (a) and (b) indicate statistically significant differences across genotypes
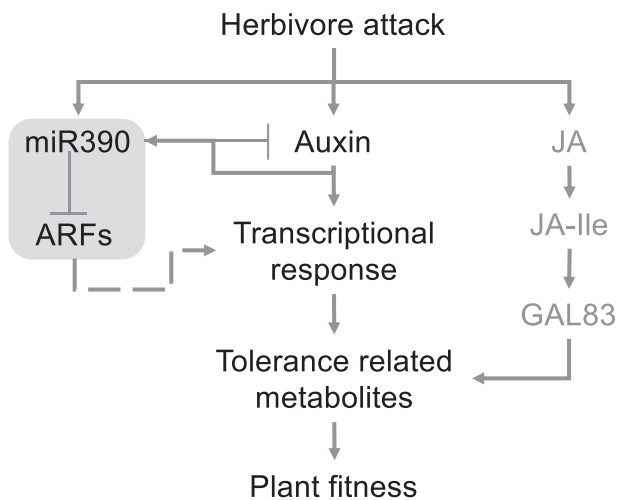

FIGURE 8 A model for miR390 function in regulating plant fitness responses during herbivory by modulating auxin but not jasmonate signaling. Dashed line: the role of ARFs in tolerance of plants to herbivory is postulated but not studied in *N. attenuata*

attacked by insects compared to susceptible plants, in a nonreciprocal manner that involves only plant response and not pest responses (Peterson et al., 2017). Tolerance is often measured in terms of reproductive output or yield (which is a currency of "fitness") of plants after herbivore attack as compared to that of unattacked plants.

Although the underlying mechanisms are largely uncharacterized, five physiological processes are thought to contribute to herbivory tolerance: alterations in photosynthesis, relative growth rate, branching or tillering, preexisting carbon reserves in roots, and the ability to relocate carbon from roots to shoots after herbivory (Koch et al., 2016; Peterson et al., 2017). At a molecular level, only a few genes, such as GAL83 SNF1-related kinase for resource allocation during the feeding of the chewing insect *M. sexta* (Schwachtje et al., 2006), peroxidases and catalases in response to chinch bug attack, and those involved in ROS detoxification mechanisms

important for Hemipteran pests tolerance, have been associated with host tolerance to herbivory (Koch et al., 2016; Peterson et al., 2017). Furthermore, ROS signaling is thought to overlap with phytohormone (JA and SA) signaling pathways, which may be key hubs through which signals might be propagated for long-term responses, leading to mitigation and resumption of growth after herbivory (Koch et al., 2016).

N. attenuata has coevolved with the attack of its specialist herbivore, *M. sexta* (Lepidoptera). This host plant deploys a suite of direct and indirect defenses which are not always effective and a *M. sexta* larvae is often able to completely defoliate its host plant. Therefore, *N. attenuata* benefits from tolerance responses as they complement the elaborate direct and indirect defense traits elicited during *M. sexta* attack (Schwachtje et al., 2006). By down-regulating *GAL83* expression in response to *M. sexta* attack, *N. attenuata* is able to shunt recently fixed photoassimilates to roots which are later remobilized to shoots to sustain reflowering and to tolerate herbivory (Schwachtje et al., 2006). Furthermore, *N. attenuata* deploys auxin signaling, in addition to jasmonate signaling, to regulate regrowth and maximize plant fitness during herbivory (Machado et al., 2013). Overexpression of miR390 reduced tolerance, as revealed by significant reductions in seed capsule production, without affecting the growth of *M. sexta* larvae. This reduced tolerance could be attributed to reductions in auxin accumulation during herbivory (for instance due to limited elicitation of *YUCCA* genes), along with reduced accumulations of *ARF4* transcripts. On the other hand, overexpression of miR390 did not affect jasmonate accumulations (or other phytohormones such as SA or ABA) or the expression of *GAL83*. A minor compensatory growth response as seen in stalk elongation was noticed in OEmiR390 plants after caterpillar feeding, but these increases failed to compensate for the reduced capsule production. The reduction in capsule production of *M. sexta* attacked OEmiR390 plants could be restored to WT levels when plants were exogenously treated with IAA.

Importantly, the mechanisms of host plant tolerance responses differ considerably according to the feeding guilds (such as chewing vs sucking), herbivore specializations (specialists or generalists), and the plants' environment, including associations with symbionts like

AM fungi (Koch et al., 2016; Peterson et al., 2017; Tao et al., 2016). In order to tolerate attack from sucking insects, plants deploy ROS-detoxification and photosynthetic rate changes, whereas attack from defoliating chewing insects engages mechanisms related to over-compensation through the production of new tissues, changes in architecture (e.g., increased branching), or resource relocation (Koch et al., 2016). Under field conditions, *N. attenuata* plants face an unpredictable level of herbivore attack every year (Baldwin, 2001; Pandey & Baldwin, 2007; Pradhan et al., 2020). The composition of the herbivore community is known to vary across years and may be responsible for the substantial amount of adaptive plasticity observed in this species (Navarro-Quezada et al., 2020). During the 2019 field season, when OEmiR390 plants were exposed to the natural herbivore community, which at the time of the experiments did not include a significant *Manduca* component, we saw only a mild fitness consequence of herbivory, likely due to the overall paucity of folivory. We predict that had *Manduca* been a significant part of the herbivore community, and the plants had suffered significant folivory, we would have observed considerable fitness differences between WT plants with their functional miR390-auxin regulatory module and the OEmiR390 lines in which this module was disabled. In order to abide by US Department of Agriculture Animal and Plant Health Inspection Service (APHIS) regulations for field release of transgenic plants, we had to terminate our study sooner than the glasshouse studies to prevent any spread of transgenic seeds in nature. Therefore, a fully detailed quantification of reproductive output of OEmiR390 plants in the field could not be made, and only an early account could be recorded. Nevertheless, this is one of the first field tests of miRNA function.

Molecularly, miR390, ARFs, and auxin form the components of an auto-regulatory circuit in a cell (Marin et al., 2010; Yoon et al., 2010). miR390 transcription has been shown to be induced at high IAA concentrations, and miR390 expression is regarded as a regulatory component that senses auxin concentrations for modulating ARF4 expression (Yoon et al., 2010). Further, positive and negative feedback regulation of miR390 by ARFs have also been proposed (Marin et al., 2010). In the context of our study, recruitment of such a regulatory circuit is highly plausible because in response to herbivore attack, IAA levels are rapidly induced (Machado et al., 2013). Herbivore attack also induces the expression of miR390 in the attacked leaves. We hypothesize that miR390 regulates the expression of ARF4, which might exert a feedback to optimize auxin sensing and in turn its biosynthesis by YUCCAs (Figure 8). miR390-modulated expression of ARF transcription factors could regulate the downstream tolerance response related to modulation of primary and secondary metabolite accumulations that are produced in response to herbivory and ultimately provide the metabolic basis for tolerance (Figure 8).

miR390 has been a widely conserved miRNA in eudicots (Xia et al., 2017) that often acts as a critical factor in auxin signaling. The miR390-ARF regulatory pathway has undergone a dynamic evolutionary route (Xia et al., 2017). Therefore, it should not be surprising that the biological functions of such a component would also undergo diversification as a consequence of changing ecological and environmental selection pressures. Nearly half of the miRNA gene families are frequently lost and the "repertoires of miRNA genes" have often "dynamically" changed during the evolution (Nozawa et al., 2012). Indeed, several divergent biological functions of miR390 have been identified in addition to its well-studied roles in developmental processes: for example, miR390 has been implicated in gall formation by *Meloidogyne* (Cabrera et al., 2016), cadmium and aluminum tolerance in rice and flax (Ding et al., 2016; Dmitriev et al., 2017), symbiotic nodulation in *Medicago* (Hobecker et al., 2017), and salt stress induced developmental plasticity of popular (He et al., 2018). Here, we extend the functional arena of miR390 to a role in herbivore induced tolerance responses in *N. attenuata*. The next step would be to gain a deeper insight into molecular mechanism of action that warrants future investigation. Further research is needed to determine how miR390 responds to herbivory signals and regulates auxin signaling to ultimately provide the observed tolerance responses.

4 | MATERIALS AND METHODS

4.1 | Plant material, generation of miR390-overexpressing plants, and growth conditions

N. attenuata wild type (WT) plants (22nd inbred generation) were transformed according to Krügel et al. (2002) using the plasmid depicted in Figure S1, carrying the miR390 precursor sequence (Figure S1). *N. attenuata* transcriptome sequencing on the GS FLX Titanium platform (Gase & Baldwin, 2012) revealed the sequence of the miR390 precursor transcript (GBGF01029632) (Bozorov et al., 2012). Based on this sequence information, we designed primers SRNA1–39 (5′-GCGGCGCTCGAGATCCATTCATTTATAGT ACATCTTTAG-3′) and SRNA2–42 (5′-GCGGCGGGTCACCGTTATC ATTGAAAGAACAGTAACATATAC-3′). For cDNA synthesis, total RNA was isolated from *N. attenuata* leaves harvested 1 h after treatment with wound and oral secretion from *M. sexta* larvae using the TRIZOL method as recommended by the manufacturer (http://www.invitrogen.com). Reverse transcription was done with SuperScript Reverse Transcriptase following the protocol of the same manufacturer. PCR was performed with the designed primer pair and Phusion DNA Polymerase (www.thermofisher.com) according to the instructions of the manufacturer to amplify the pre-miR390 gene from the synthesized cDNA. The amplified PCR fragment (Figure S1) was then cloned in the 9.7 kb XhoI-BstEII fragment of the binary plant transformation vector pRESC800 (Gase & Baldwin, 2012); JQ354897), yielding pRESC9MIR390. T1 seeds of 20 independently transformed lines were screened on hygromycin according to (Gase et al., 2011). The number of insertions was checked by evaluating the number of reads of different target sites of the transformation vector as well as three internal genes using the nCounter Nanostring procedure, as previously described (He et al., 2019). Lines "385–42" and "392–63" showed a single complete insertion (Figure S1).

For glasshouse experiments, WT seeds (31st inbred generation) were germinated on GB5 medium and OEmiR390 lines (A-12-392-63-71, A-12-385-42-51) were germinated on GB5

PRADHAN ET AL.

American Society
of Plant Biologists

SEB
SOCIETY FOR EXPERIMENTAL BIOLOGY

WILEY | 11 of 14

supplemented with hygromycin (Krügel et al., 2002; Onkokesung et al., 2012); 10–12 days after germination, plants were transferred to Teku pots either filled with soil or sand for the AMF experiment (Krügel et al., 2002; Pandey et al., 2018); 10–12 days later plants were transferred to soil or AMF inoculum (active AMF inoculum, Biomyc Vital, www.biomyc.de, diluted 1:10 with expanded clay, particle size: 2–4 mm). Plants were grown either as single plants in 1-L pots or under competition with a size- and age-matched WT neighbor (Pandey et al., 2008), as indicated in the text. Plants grown in soil received the optimal amount of nutrients, while AMF inoculated plants were fertilized with hydroponic solution with 1/10 of the regular Pi content during rosette stage, and starting with the elongation stage with 1/4 Pi concentration (Pandey et al., 2018).

Plant performance measurements of rosette diameter, chlorophyll content, stalk length, flower number, total capsule number, and shoot and root fresh mass was recorded at respective time points.

4.2 | miR390 accumulation and transcripts measurements by quantitative real-time PCR

Overexpression of miR390 was evaluated by quantitative real-time PCR (qPCR) assays, as was the abundance of *YUCCCA1*, *YUCCA3*, *ARF2–4*, and *GAL83* transcripts. Total RNA was extracted from frozen seedlings using the lithium chloride method (Kistner & Matamoros, 2005) and adapted to *N. attenuata* (Pradhan et al., 2017), and DNA traces were removed with DNase I (DNA-free kit; Ambion). For analysis of miRNA abundances, a total of 1 μg of total RNA was converted to complementary miRNA using miScript® II RT Kit (Qiagen, Cat. No.- 218,161) according to the manufacturer's instruction (www.qiagen.com). qPCR was performed with the help of miScript SYBR Green PCR kit (Qiagen, Cat. No. 218073), by following the manufacturer's protocol, adapted to *N. attenuata* and previously described (Pradhan et al., 2020), where 10 ng of complimentary miRNA was used. For analysis of targets, 1 μg of total RNA was converted to cDNA according to the manufacturer's instruction using the SuperScript Reverse Transcriptase (Invitrogen). Using 10–50 ng of cDNA, qPCR was performed with the qPCR core kit for Taykon™ SYBR master mix (Eurogentec) on a Mx3005P qPCR system (Stratagene, Santa Clara, CA, USA; http://www.stratagene.com). The $2^{-\Delta\Delta CT}$ method was used for data analysis, and the 5S rRNA gene was used for normalization of miRNA (Pradhan et al., 2020), whereas the ECI gene was used for normalization of *YUCCA*, *ARF*, and *GAL83* transcripts (Bubner et al., 2004). Sequences of all primers (genes and miRNAs) used in the study are provided in Table S1.

4.3 | Blumenol analysis to estimate root colonization by AMF

11-Carboxyblumenol-C-glucoside is a reliable quantitative leaf marker for root arbuscule colonization (Wang et al., 2018). Leaf samples were powdered with two steel balls with an automated tissue homogenizer

(SPEX SamplePrep) for 60 s at 1150 strokes min^{-1}. About 100 mg plant tissues were extracted with 800 μl of 80% MeOH spiked with internal standard (10 ng ABA per sample). After shaking in the tissue homogenizer, samples were centrifuged for 20 min with 1913 × g at 4°C; the supernatant was collected and analyzed by ultrahigh performance liquid chromatography (UHPLC) coupled to a triple quadrupole mass spectrometer equipped with a heated electrospray ionization (HESI) source (EVOQ, Bruker, Bremen, Germany) as described previously (Mindt et al., 2019; Wang et al., 2018).

4.4 | Determination of susceptibility against *Fusarium brachygibbosum*

The *F. brachygibbosum* pathogenesis bioassay was conducted as previously described (Pradhan et al., 2020). The Padwick Utah 4 strain, isolated from diseased *N. attenuata* plants growing in the native habitats (Schuck et al., 2014), was used for determining whether the susceptibility of OEmiR390 plants to a natural pathogen was altered. A pure fungal culture was regularly maintained on potato dextrose agar (PDA, Fluka Analytical, Steinheim, Germany) at 25°C in the dark (Pradhan et al., 2020). A droplet (10 μl) of spore suspension (10^6 spore ml^{-1}) of *F. brachygibbosum*, harvested from 12- to 15-day-old pure cultures grown on PDA, was inoculated on the "+2-leaves" of rosette-stage (Pradhan et al., 2020) *N. attenuata* plants under high humidity in a climate controlled growth chamber (day/night cycle of 16 h (26°C)/8 h (22°C) with 80 ± 5% humidity. First disease symptoms were visible within 3–4 dpi and lesion size was measured at 5 dpi (Pradhan et al., 2020); 10–15 independent biological replicates per genotype were used.

4.5 | Herbivore performance assay

M. sexta performance assays were conducted on stably transformed lines as described earlier (Pandey & Baldwin, 2007; Pradhan et al., 2017); 20 replicate plants of WT and the two OEmiR390 lines were germinated, transferred to Teku pots and grown on soil in 1-L pots in the glasshouse as described above. Two neonate larvae were placed on the lower surface of the +2 leaf of rosette stage plants; after 2 days, one neonate larva per plant was allowed to feed for 11 to 14 days. Caterpillar biomass was recorded every 3 to 4 d. Rosette size and stalk length were recorded weekly. All capsules per plant were counted 9, 10, and 11 weeks after potting. Closed (unripe) and open (ripe) capsules were counted separately. The caterpillar performance assay and growth and fitness measurements were repeated in an independent biological experiment with a similar setup using 10 independent biological replicates.

4.6 | Auxin complementation assays

For auxin complementation assays, 1 mM IAA (Pandey et al., 2008) was exogenously supplied to herbivore-attacked plants. Fully

expanded WT and OEmiR390 plants were subject to *M. sexta* neonates as described above. After 3 days of caterpillar feeding, IAA, dissolved in lanolin paste (.1752 mg/ml) and 20 μl/petiole of this IAA-lanolin paste was applied to the petioles of +2 leaves as previously described (Machado et al., 2013). Plants were grown until seed set. Recovery of plant fitness was evaluated by counting seed capsules as described above.

4.7 | Quantification of phytohormones and secondary metabolites

To determine differences in herbivore-induced phytohormone and secondary metabolite accumulation between the WT and OEmiR390 plants, leaves were harvested after continuous caterpillar feeding for 9 days, immediately frozen in liquid nitrogen and stored at −80°C until further processing. Leaf material was ground into a fine powder and 100 mg of the frozen tissue were aliquoted into 96-well biotubes and samples were extracted following a published protocol (Schäfer et al., 2016). After solid phase extraction samples were reconstituted in acidified MeOH (.2 N formic acid [FA] in 80% MeOH) and analyzed on an UHPLC-ESI-Triple-Quadrupole-MS (EVOQ Elite, Bruker) using a Zorbax Eclipse XDB-C18 column (100 x 2 mm, particle size 1.8 μm, Agilent) as previously described (Schäfer et al., 2016). Post-run data analysis was performed in the MS Data Review software (Bruker). Compound concentrations were calculated using the corresponding labeled internal standards as previously described (Schäfer et al., 2016).

A second aliquot (100 mg) of the frozen leaf material was extracted in 800 μl of 80% MeOH containing the internal standard testosterone and used for a qTOF analysis. After incubation for 30 min at −20°C, samples were homogenized in a Genogrider (60 s at 1150 strokes min^{-1}), centrifuged at 1913× g for 20 min at 4°C and 150 μl of supernatant were transferred to a skirted 96-well plate and subsequently sealed with sticky film. Separation was performed using a UHPLC system (UltiMate3000 RSLC, Thermo Scientific) equipped with a 150 mm × 2.1 mm, 2.2 μm, Acclaim RSLC C18 column (Thermo-Fisher). The following binery solvent gradient (A: water, .1% [v/v] acetonitrile, .05%FA; and B: acetonitrile, .05% FA) was applied: 0 to .5 min, isocratic 90% A, 10% B; .5 to 23.5 min, linear ramp to 10% A, 90% B; 23.5 to 25 min, isocratic 10% A, 90% B. The flow rate was .4 ml min^{-1} and 2 μl of leaf extract were injected. Mass detection was carried out on a Bruker ESI-qTOF-MS as previously described (Gaquerel et al., 2010). Post-run analysis was performed in the Compass DataAnalysis software (Bruker).

4.8 | Field experiments

For field-grown plants, seeds of the transformed *N. attenuata* lines (OEmiR390, EV) were imported and released under US Department of Agriculture Animal and Plant Health Inspection Service (APHIS) notification numbers 18–282-103r with genotypic descriptors NA418 and NA056, respectively. The field experiment was conducted at the Lytle Ranch Preserve, located in the Great Basin Desert of Southwestern Utah, USA (latitude 37.146, longitude 114.020). WT and OEmiR390 (A-12-392-63-71) seeds were germinated directly on borax-soaked Jiffy 703 pots (AlwaysGrows), and transplanted into the field plot 3 to 4 weeks later. The two genotypes were grown in pairs; in total 18 replicate plants per genotype were analyzed. Rosette diameter, stalk length, flower number and the number of immature seed capsules were determined at the indicated time-points. Seed capsules were removed after counting to fulfill safety regulations. Herbivore damage per plant was estimated 3, 4, and 7 weeks after planting.

CONFLICT OF INTEREST

The authors declare no conflict of interests.

AUTHOR CONTRIBUTIONS

S.P.P. and I.T.B. conceived the research plan and designed experiments, M.P., C.R., R.H. and S.P.P. conducted research and analyzed data, S.P.P. and I.T.B. conducted field work. S.P.P., M.P. and I.T.B wrote the article with contributions from C.R. and R.H., I.T.B. provided most of the resources.

ORCID

Maitree Pradhan https://orcid.org/0000-0002-9279-640X
Catarina Rocha https://orcid.org/0000-0002-4379-3149
Rayko Halitschke https://orcid.org/0000-0002-1109-8782
Ian T. Baldwin https://orcid.org/0000-0001-5371-2974
Shree P. Pandey https://orcid.org/0000-0002-4546-9123

REFERENCES

Axtell, M. J., Jan, C., Rajagopalan, R., & Bartel, D. P. (2006). A two-hit trigger for siRNA biogenesis in plants. *Cell*, *127*, 565–577. https://doi.org/10.1016/j.cell.2006.09.032

Baldwin, I. T. (2001). An ecologically motivated analysis of plant-herbivore interactions in native tobacco. *Plant Physiology*, *127*, 1449–1458. https://doi.org/10.1104/pp.010762

Bozorov, T. A., Baldwin, I. T., & Kim, S.-G. (2012). Identification and profiling of miRNAs during herbivory reveals jasmonate-dependent and -independent patterns of accumulation in *Nicotiana attenuata*. *BMC*

Plant Biology, *12*, 209–209. https://doi.org/10.1186/1471-2229-12-209

Brant, E. J., & Budak, H. (2018). Plant small non-coding RNAs and their roles in biotic stresses. *Frontiers in Plant Science*, *9*, 1038–1038. https://doi.org/10.3389/fpls.2018.01038

Bubner, B., Gase, K., & Baldwin, I. T. (2004). Two-fold differences are the detection limit for determining transgene copy numbers in plants by real-time PCR. *BMC Biotechnology*, *4*, 1–14. https://doi.org/10.1186/1472-6750-4-14

Cabrera, J., Barcala, M., García, A., Rio-Machín, A., Medina, C., Jaubert-Possamai, S., Favery, B., Maizel, A., Ruiz-Ferrer, V., Fenoll, C., & Escobar, C. (2016). Differentially expressed small RNAs in Arabidopsis galls formed by Meloidogyne javanica: A functional role for miR390 and its TAS3-derived tasiRNAs. *The New Phytologist*, *209*, 1625–1640. https://doi.org/10.1111/nph.13735

Cho, S. H., Coruh, C., & Axtell, M. J. (2012). miR156 and miR390 regulate tasiRNA accumulation and developmental timing in *Physcomitrella patens*. *Plant Cell*, *24*, 4837–4849. https://doi.org/10.1105/tpc.112.103176

Cuperus, J. T., Fahlgren, N., & Carrington, J. C. (2011). Evolution and functional diversification of MIRNA genes. *Plant Cell*, *23*, 431–442. https://doi.org/10.1105/tpc.110.082784

Ding, Y., Ye, Y., Jiang, Z., Wang, Y., & Zhu, C. (2016). MicroRNA390 is involved in cadmium tolerance and accumulation in Rice. *Frontiers in Plant Science*, *7*, 235–235. https://doi.org/10.3389/fpls.2016.00235

Dmitriev, A. A., Kudryavtseva, A. V., Bolsheva, N. L., Zyablitsin, A. V., Rozhmina, T. A., Kishlyan, N. V., Krasnov, G. S., Speranskaya, A. S., Krinitsina, A. A., Sadritdinova, A. F., Snezhkina, A. V., Fedorova, M. S., Yurkevich, O. Y., Muravenko, O. V., Belenikin, M. S., & Melnikova, N. V. (2017). miR319, miR390, and miR393 are involved in aluminum response in flax (*Linum usitatissimum* L.). *BioMed Research International*, *2017*, 4975146.

Gaquerel, E., Heiling, S., Schoettner, M., Zurek, G., & Baldwin, I. T. (2010). Development and validation of a liquid chromatography—electrospray ionization—time-of-flight mass spectrometry method for induced changes in *Nicotiana attenuata* leaves during simulated herbivory. *Journal of Agricultural and Food Chemistry*, *58*, 9418–9427. https://doi.org/10.1021/jf1017737

Gase, K., & Baldwin, I. T. (2012). Transformational tools for next-generation plant ecology: Manipulation of gene expression for the functional analysis of genes. *Plant Ecology and Diversity*, *5*, 485–490. https://doi.org/10.1080/17550874.2012.754797

Gase, K., Weinhold, A., Bozorov, T., Schuck, S., & Baldwin, I. T. (2011). Efficient screening of transgenic plant lines for ecological research. *Molecular Ecology Resources*, *11*, 890–902. https://doi.org/10.1111/j.1755-0998.2011.03017.x

He, F., Xu, C., Fu, X., Shen, Y., Guo, L., Leng, M., & Luo, K. (2018). The *MicroRNA390/TRANS-ACTING SHORT INTERFERING RNA3* module mediates lateral root growth under salt stress via the Auxin pathway. *Plant Physiology*, *177*, 775–791. https://doi.org/10.1104/pp.17.01559

He, H., He, L., & Gu, M. (2014). Role of microRNAs in aluminum stress in plants. *Plant Cell Reports*, *33*, 831–836. https://doi.org/10.1007/s00299-014-1565-z

He, J., Fandino, R. A., Halitschke, R., Luck, K., Köllner, T. G., Murdock, M. H., Ray, R., Gase, K., Knaden, M., Baldwin, I. T., & Schuman, M. C. (2019). An unbiased approach elucidates variation in (S)-(+)-linalool, a context-specific mediator of a tri-trophic interaction in wild tobacco. *Proceedings of the National Academy of Sciences*, *116*, 14651–14660. https://doi.org/10.1073/pnas.1818585116

Hobecker, K. V., Reynoso, M. A., Bustos-Sanmamed, P., Wen, J., Mysore, K. S., Crespi, M., Blanco, F. A., & Zanetti, M. E. (2017). The microRNA390/TAS3 pathway mediates symbiotic nodulation and lateral root growth. *Plant Physiology*, *174*, 2469–2486. https://doi.org/10.1104/pp.17.00464

Howe, G. A., & Jander, G. (2008). Plant immunity to insect herbivores. *Annual Review of Plant Biology*, *59*, 41–66. https://doi.org/10.1146/annurev.arplant.59.032607.092825

Kaur, H., Shaker, K., Heinzel, N., Ralph, J., Gális, I., & Baldwin, I. T. (2012). Environmental stresses of field growth allow cinnamyl alcohol dehydrogenase-deficient *Nicotiana attenuata* plants to compensate for their structural deficiencies. *Plant Physiology*, *159*, 1545–1570. https://doi.org/10.1104/pp.112.196717

Kessler, A., Halitschke, R., & Baldwin, I. T. (2004). Silencing the jasmonate cascade: Induced plant defenses and insect populations. *Science*, *305*, 665–668. https://doi.org/10.1126/science.1096931

Kistner, C., & Matamoros, M. (2005). RNA isolation using phase extraction and LiCl precipitation. In A. J. Márquez, J. Stougaard, M. Udvardi, M. Parniske, H. Spaink, G. Saalbach, J. Webb, M. Chiurazzi, & A. J. Márquez (Eds.), *Lotus Japonicus Handbook* (pp. 123–124). Netherlands: Springer.

Koch, K. G., Chapman, K., Louis, J., Heng-Moss, T., & Sarath, G. (2016). Plant tolerance: A unique approach to control Hemipteran pests. *Frontiers in Plant Science*, *7*, 1363. https://doi.org/10.3389/fpls.2016.01363

Krügel, T., Lim, M., Gase, K., Halitschke, R., & Baldwin, I. T. (2002). *Agrobacterium*-mediated transformation of *Nicotiana attenuata*, a model ecological expression system. *Chemoecology*, *12*, 177–183. https://doi.org/10.1007/PL00012666

Li, S., Castillo-González, C., Yu, B., & Zhang, X. (2017). The functions of plant small RNAs in development and in stress responses. *The Plant Journal*, *90*, 654–670. https://doi.org/10.1111/tpj.13444

Lu, Y., Feng, Z., Liu, X., Bian, L., Xie, H., Zhang, C., Mysore, K. S., & Liang, J. (2018). MiR393 and miR390 synergistically regulate lateral root growth in rice under different conditions. *BMC Plant Biology*, *18*, 261. https://doi.org/10.1186/s12870-018-1488-x

Machado, R. A. R., Ferrieri, A. P., Robert, C. A. M., Glauser, G., Kallenbach, M., Baldwin, I. T., & Erb, M. (2013). Leaf-herbivore attack reduces carbon reserves and regrowth from the roots via jasmonate and auxin signaling. *New Phytologist*, *200*, 1234–1246. https://doi.org/10.1111/nph.12438

Machado, R. A. R., Robert, C. A. M., Arce, C. C. M., Ferrieri, A. P., Xu, S., Jimenez-Aleman, G. H., Baldwin, I. T., & Erb, M. (2016). Auxin is rapidly induced by herbivore attack and regulates a subset of systemic, jasmonate-dependent defenses. *Plant Physiology*, *172*, 521–532. https://doi.org/10.1104/pp.16.00940

Marin, E., Jouannet, V., Herz, A., Lokerse, A. S., Weijers, D., Vaucheret, H., Nussaume, L., Crespi, M. D., & Maizel, A. (2010). miR390, *Arabidopsis TAS3* tasiRNAs, and their *AUXIN RESPONSE FACTOR* targets define an autoregulatory network quantitatively regulating lateral root growth. *Plant Cell*, *22*, 1104–1117. https://doi.org/10.1105/tpc.109.072553

Mindt, E., Wang, M., Schäfer, M., Halitschke, R., & Baldwin, I. T. (2019). Quantification of blumenol derivatives as leaf biomarkers for plant-AMF association. *Bio-Protocol*, *9*, e3301. https://doi.org/10.21769/BioProtoc.3301

Morozov, S. Y., Milyutina, I. A., Erokhina, T. N., Ozerova, L. V., Troitsky, A. V., & Solovyev, A. G. (2018). TAS3 miR390-dependent loci in non-vascular land plants: Towards a comprehensive reconstruction of the gene evolutionary history. *PeerJ*, *6*, e4636. https://doi.org/10.7717/peerj.4636

Navarro-Quezada, A., Gase, K., Singh, R. K., Pandey, S. P., & Baldwin, I. T. (2020). *Nicotiana attenuata* genome reveals genes in the molecular machinery behind remarkable adaptive phenotypic plasticity. In N. V. Ivanov, N. Sierro, & M. C. Peitsch (Eds.), *The tobacco plant genome* (pp. 211–229). Cham: Springer International Publishing. https://doi.org/10.1007/978-3-030-29493-9_13

Nozawa, M., Miura, S., & Nei, M. (2012). Origins and evolution of MicroRNA genes in plant species. *Genome Biology and Evolution*, *4*, 230–239. https://doi.org/10.1093/gbe/evs002

Onkokesung, N., Gaquerel, E., Kotkar, H., Kaur, H., Baldwin, I. T., & Galis, I. (2012). MYB8 controls inducible phenolamide levels by activating three novel hydroxycinnamoyl-coenzyme A: Polyamine transferases in *Nicotiana attenuata*. *Plant Physiology*, *158*, 389–407. https://doi.org/10.1104/pp.111.187229

Pandey, P., Srivastava, P. K., & Pandey, S. P. (2019). Prediction of plant miRNA targets. In *Plant MicroRNAs* (pp. 99–107). New York, NY: Humana Press.

Pandey, P., Wang, M., Baldwin, I. T., Pandey, S. P., & Groten, K. (2018). Complex regulation of microRNAs in roots of competitively-grown isogenic *Nicotiana attenuata* plants with different capacities to interact with arbuscular mycorrhizal fungi. *BMC Genomics*, *19*, 937. https://doi.org/10.1186/s12864-018-5338-x

Pandey, S. P., & Baldwin, I. T. (2007). RNA-directed RNA polymerase 1 (RdR1) mediates the resistance of *Nicotiana attenuata* to herbivore attack in nature. *The Plant Journal*, *50*, 40–53. https://doi.org/10.1111/j.1365-313X.2007.03030.x

Pandey, S. P., Gaquerel, E., Gase, K., & Baldwin, I. T. (2008). RNA-directed RNA polymerase3 from *Nicotiana attenuata* is required for competitive growth in natural environments. *Plant Physiology*, *147*, 1212–1224. https://doi.org/10.1104/pp.108.121319

Peterson, R. K. D., Varella, A. C., & Higley, L. G. (2017). Tolerance: The forgotten child of plant resistance. *PeerJ*, *5*, e3934. https://doi.org/10.7717/peerj.3934

Pradhan, M., Pandey, P., Baldwin, I. T., & Pandey, S. P. (2020). Argonaute4 modulates resistance to *Fusarium brachygibbosum* infection by regulating jasmonic acid signaling. *Plant Physiology*, *184*, 1128–1152. https://doi.org/10.1104/pp.20.00171

Pradhan, M., Pandey, P., Gase, K., Sharaff, M., Singh, R. K., Sethi, A., Baldwin, I. T., & Pandey, S. P. (2017). Argonaute 8 (AGO8) mediates the elicitation of direct defenses against herbivory. *Plant Physiology*, *175*, 927–946. https://doi.org/10.1104/pp.17.00702

Santin, F., Bhogale, S., Fantino, E., Grandellis, C., Banerjee, A. K., & Ulloa, R. M. (2017). Solanum tuberosum StCDPK1 is regulated by miR390 at the posttranscriptional level and phosphorylates the auxin efflux carrier StPIN4 in vitro, a potential downstream target in potato development. *Physiologia Plantarum*, *159*, 244–261. https://doi.org/10.1111/ppl.12517

Schäfer, M., Brütting, C., Baldwin, I. T., & Kallenbach, M. (2016). High-throughput quantification of more than 100 primary- and secondary-metabolites, and phytohormones by a single solid-phase extraction based sample preparation with analysis by UHPLC–HESI–MS/MS. *Plant Methods*, *12*, 30. https://doi.org/10.1186/s13007-016-0130-x

Schuck, S., Weinhold, A., Luu, V. T., & Baldwin, I. T. (2014). Isolating fungal pathogens from a dynamic disease outbreak in a native plant population to establish plant-pathogen bioassays for the ecological model plant *Nicotiana attenuata*. *PLoS ONE*, *9*, e102915. https://doi.org/10.1371/journal.pone.0102915

Schwachtje, J., Minchin, P. E. H., Jahnke, S., van Dongen, J. T., Schittko, U., & Baldwin, I. T. (2006). SNF1-related kinases allow plants to tolerate herbivory by allocating carbon to roots. *Proceedings of the National Academy of Sciences*, *103*, 12935–12940. https://doi.org/10.1073/pnas.0602316103

Song, X., Li, Y., Cao, X., & Qi, Y. (2019). MicroRNAs and their regulatory roles in plant–environment interactions. *Annual Review of Plant Biology*, *70*, 489–525. https://doi.org/10.1146/annurev-arplant-050718-100334

Tao, L., Ahmad, A., de Roode, J. C., & Hunter, M. D. (2016). Arbuscular mycorrhizal fungi affect plant tolerance and chemical defences to herbivory through different mechanisms. *Journal of Ecology*, *104*, 561–571. https://doi.org/10.1111/1365-2745.12535

Wang, M., Schäfer, M., Li, D., Halitschke, R., Dong, C., McGale, E., Paetz, C., Song, Y., Li, S., Dong, J., Heiling, S., Groten, K., Franken, P., Bitterlich, M., Harrison, M. J., Paszkowski, U., & Baldwin, I. T. (2018). Blumenols as shoot markers of root symbiosis with arbuscular mycorrhizal fungi. *eLife*, *7*, e37093. https://doi.org/10.7554/eLife.37093

Xia, R., Xu, J., & Meyers, B. C. (2017). The emergence, evolution, and diversification of the miR390-*TAS3-ARF* pathway in land plants. *Plant Cell*, *29*, 1232–1247. https://doi.org/10.1105/tpc.17.00185

Xu, S., Brockmöller, T., Navarro-Quezada, A., Kuhl, H., Gase, K., Ling, Z., Zhou, W., Kreitzer, C., Stanke, M., Tang, H., Lyons, E., Pandey, P., Pandey, S. P., Timmermann, B., Gaquerel, E., & Baldwin, I. T. (2017). Wild tobacco genomes reveal the evolution of nicotine biosynthesis. *Proc Natl Acad Sci USA*, *114*, 6133–6138. https://doi.org/10.1073/pnas.1700073114

Yoon, E. K., Yang, J. H., Lim, J., Kim, S. H., Kim, S.-K., & Lee, W. S. (2010). Auxin regulation of the microRNA390-dependent transacting small interfering RNA pathway in Arabidopsis lateral root development. *Nucleic Acids Research*, *38*, 1382–1391. https://doi.org/10.1093/nar/gkp1128

SUPPORTING INFORMATION

Additional supporting information may be found in the online version of the article at the publisher's website.